NITROGEN DOPED TITANIA-PHOSPHORYLATED CHITOSAN FOR THE PHOTOCATALYTIC DECONTAMINATION OF SYNTHETIC DYES

SUMALINY A/P SUBRAMANIAM

UNIVERSITI SAINS MALAYSIA

2024

NITROGEN DOPED TITANIA-PHOSPHORYLATED CHITOSAN FOR THE PHOTOCATALYTIC DECONTAMINATION OF SYNTHETIC DYES

by

SUMALINY A/P SUBRAMANIAM

Thesis submitted in fulfilment of the requirements
for the degree of
Master of Science

July 2024

ACKNOWLEDGEMENT

My first and foremost unlimited gratitude is to the Almighty Father, because without His incognito help, none of my project could be done successfully. Despite COVID-19 that has hit nationwide, I could complete my lab work, with Him by my side, efficiently, even though there was a slight delay. My special and sincere gratitude goes to my supervisor, Dr. Sumiyyah Sabar, who have been the greatest supervisor that I have ever had. My journey was very smooth, smooth, thanks to Dr. Sumiyyah's advice, criticismd motivational support. The present work has been financially supported by RUI Grant (1001/PJJAUH/8011028). My sincere appreciation also goes to my co-supervisor, Dr. Foo Keng Yuen for his limitless support and guidance. A special thanks to all the laboratory personnel especially Mr. Azhar, Mr. Yushamdan, Mr. Mutalib, Mr. Sivaraj, Mr. Zamri, Mr. Sujay, Mrs. Ami Mardiana and Mrs. Wan Zulilawati for their prompt analytical instrument services. A special thanks goes to my labmate, Nur Syazwani Mubarak for her unlimited advises and discussions throughout my MSc journey. I would like to take this opportunity to express my sincere thanks to all the lecturers and staffs of School of Distance Education and Institute of Postgraduate Studies (IPS) for lending a help at the appropriate time. Last but not least, I would like to take this opportunity to thank my parents, Subramaniam and Mahalakshmy, my siblings, Thivyaa, Sandra and Mugi, my spiritual siblings Aishu, Wahyu and Keerthana, and my friends Syahira Idayu, Leong Kar Xin and Sam Ka Kei for their unlimited support, love and blessings which had brought me to the success in my life.

TABLE OF CONTENTS

ACKNOWLEDGEMENT ..... **ii**

TABLE OF CONTENTS ..... **iii**

LIST OF TABLES ..... **viii**

LIST OF FIGURES ..... **ix**

LIST OF SYMBOLS ..... **xii**

LIST OF ABBREVIATIONS ..... **xiii**

LIST OF APPENDICES ..... **xiii**

ABSTRAK ..... **xvi**

ABSTRACT ..... **xviii**

CHAPTER 1 INTRODUCTION **1**

1.1 Overview 1

1.2 Problem statement 7

1.3 Research objectives 9

1.4 Scope of study 9

1.5 Outline of thesis 10

CHAPTER 2 LITERATURE REVIEW **11**

2.1 Advanced oxidation processes 11

2.1.1 Photocatalysis 15

2.1.2 Principles of heterogeneous photocatalysis 16

2.1.3 Kinetic Modelling 18

2.2 Adsorption 19

2.3 Titanium dioxide (TiO_2) 21

2.3.1 General 21

2.3.2 Properties of TiO_2 semiconductor 21

2.3.3 TiO_2 in photocatalysis 22

2.3.4 Mineralization 25
2.3.5 Limitations of TiO_2 photocatalyst 25
2.4 Modification of TiO_2 26
2.4.1 Combination with adsorbents 26
2.4.2 Doping with non-metal atoms 28
2.4.3 Doping with metal ions 30
2.4.4 Sensitization 32
2.4.5 Heterojunction 34
2.5 Chitosan (CS) biopolymer 36
2.5.1 Properties of CS 37
2.5.2 Application of CS 40
2.5.3 Limitations of CS 41
2.5.4 Modification of CS 42
2.5.4(a) Physical modification 43
2.5.4(b) Chemical modification 44
2.6 Combination of TiO_2 and chitosan for water 46
2.7 Dye pollution 47
2.7.1 Acid Red 88 (AR88) dye 47
2.7.2 Methylene Blue (MB) dye 49
CHAPTER 3 METHODOLOGY 50
3.1 Chemicals and reagents 50
3.2 Instruments and equipment 51
3.3 Preparation of dye aqueous solution 52
3.4 Preparation of phosphorylated chitosan (PCS) 52
3.5 Preparation of nitrogen doped titania (NT) 53
3.6 Preparation of nitrogen doped titania-phosphorylated chitosan (NTP) 54
3.7 Characterization of nanocomposite 54

3.7.1 Scanning electron microscope coupled with energy dispersive X-ray spectrometer (SEM-EDX) 54
3.7.2 Fourier transform infrared spectroscopy (FTIR) 55
3.7.3 X-ray diffraction (XRD) analysis 55
3.7.4 Surface area and porosity analysis 56
3.7.5 Thermal gravimetric analysis (TGA) 56
3.7.6 Ultraviolet–Visible Diffuse Reflectance Spectroscopy (UV–Vis DRS) 56
3.7.7 X-ray photoelectron spectroscopy (XPS) 57
3.7.8 Determination of point of zero charge (pH_{pzc}) 57
3.8 Batch adsorption studies of PCS 57
3.8.1 Effect of solution pH 58
3.8.2 Effect of initial dye concentration and contact time 58
3.9 Adsorption isotherms 59
3.10 Adsorption kinetics 59
3.11 Thermodynamics 59
3.12 Reusability of PCS 60
3.13 Photocatalytic degradation 60
3.13.1 Mass ratio studies 61
3.13.2 Dosage 62
3.13.3 Effect of pH solution 62
3.13.4 Effect of initial dye concentration and contact time 62
3.14 Reusability of NTP 63
3.15 Radical scavengers 63
3.16 Mineralization 64
3.16.1 Total organic carbon (TOC) analysis 64
3.16.2 Ionic chromatography (IC) analysis 64

CHAPTER 4 RESULT AND DISCUSSION..... 66

4.1 Preparation of PCS 66

4.2 Characterization of PCS 66

4.2.1 SEM-EDX analysis 66

4.2.2 FTIR analysis 68

4.2.3 Pore structural analysis 70

4.2.4 XRD analysis 70

4.2.5 Determination of pH_{pzc}.....71

4.3 Adsorption of AR88 by PCS 72

4.3.1 Effect of pH.....72

4.3.2 Effect of initial dye concentration and contact time 74

4.3.3 Adsorption kinetics 75

4.3.4 Adsorption isotherm.....78

4.3.5 Diffusion models.....84

4.3.6 Thermodynamics.....86

4.3.7 Reusability of PCS 88

4.4 Preparation of nitrogen doped titania (NT) 89

4.4.1 Mass ratio of nitrogen and titania content.....89

4.5 Preparation of nitrogen doped titania-phosphorylated chitosan (NTP) 91

4.5.1 Effect of PCS loading 91

4.6 Characterization of photocatalyst.....93

4.6.1 SEM-EDX analysis 93

4.6.2 FTIR analysis 95

4.6.3 Pore structural analysis 96

4.6.4 UV-visible diffuse reflectance spectroscopy (DRS).....97

4.6.5 XRD analysis 100

4.6.6 TGA analysis.....101

4.6.7 XPS analysis 103
4.6.8 Determination of pH_{pzc} 105
4.7 Photocatalytic studies 106
4.7.1 Control experiment 106
4.7.2 Effect of dosage 108
4.7.3 Effect of initial pH of solution 110
4.7.4 Effect of initial concentration and contact time 113
4.8 Langmuir-Hinshelwood kinetic model 115
4.9 Reusability studies 118
4.10 Radical scavengers 119
4.11 Mineralisation 121
4.11.1 TOC analysis 121
4.11.2 IC analysis 123
CHAPTER 5 CONCLUSION AND FUTURE RECOMMENDATIONS ... 127
5.1 Conclusion 127
5.2 Recommendations for Future Research 129
REFERENCES 130
APPENDICES
LIST OF PUBLICATIONS, CONFERENCE AND EXHIBITION

LIST OF TABLES

Page

Table 2.1 The advantages and disadvantages of various AOP (Brienza & Katsoyiannis, 2017) 13

Table 2.2 Intrinsic properties of CS (Gregorio Crini & Badot, 2008) 40

Table 2.3 Benefits and drawbacks of modification methods of chitosan (Jianlong Wang & Zhuang, 2022) 43

Table 4.1 Elemental analysis and surface properties of CS and PCS 69

Table 4.2 Surface properties of CS and PCS 71

Table 4.3 Adsorption kinetic model parameters onto AR88 adsorption onto P-CS at different initial dye concentrations 79

Table 4.4 The isotherm parameters of the Langmuir, Freundlich, and Temkin isotherm models for AR88 adsorption onto P-CS 82

Table 4.5 A comparison of AR88 maximum adsorption capacity, qm, on various adsorbents 83

Table 4.6 Thermodynamics parameters for the adsorption of AR88 by PCS 88

Table 4.7 Properties of TiO_2, NT, NTP and NTP after photocatalysis 96

Table 4.8 Surface properties of CS and PCS 98

Table 4.9 The absorption edge, λ, and band gap of the catalysts. 101

Table 4.10 The values of rate constant, k, according to its respective initial dye concentrations. 118

Table 4.11 The values of r^2, k and k according to their respective initial dye concentrations. 118

LIST OF FIGURES

Page

Figure 2.1 Classifications of AOPs (Poyatos *et. al.*, 2010) 16

Figure 2.2 Heterogeneous photocatalysis applications 18

Figure 2.3 Illustration of photocatalytic activity of TiO_2 mechanism on pollutant (RH) (Dong *et. al.*, 2015) 25

Figure 2.4 Schematic energy level diagram of (a) unmodified TiO_2 and (b) N-doped TiO_2 31

Figure 2.5 Schematic diagram of the mechanism of process of dye sensitization onto the surface of TiO_2 (Diaz-Angulo *et.al.*, 2019) 35

Figure 2.6 Molecular structure of Acid Red 88 (AR 88) 49

Figure 2.7 Molecular structure of Methylene Blue (MB) 50

Figure 3.1 Preparation of phosphorylated chitosan (PCS) 54

Figure 4.1 SEM images and EDX analysis of (a) CS, (b) PCS before and (c) after AR88 adsorption at 10 000× magnification 68

Figure 4.2 FTIR spectra of (a) CS, (b) PCS before, and (c) after AR88 adsorption 70

Figure 4.3 XRD profile of (a) CS and (b) PCS 771

Figure 4.4 pH_{pzc} of PCS 73

Figure 4.5 Effect of pH on the adsorptive uptake of AR88 at 30 °C, with the dosage of 20 mg, an initial dye concentration of 100 mg L^{-1} and contact time of 24 h 74

Figure 4.6 The effect of initial dye concentration and contact time on AR88 adsorptive uptake onto PCS, at 20 mg dosage and temperature of 303 K 76

Figure 4.7 Plots of (a) intraparticle diffusion and (b) Boyd models for the adsorption of AR88 by PCS 86

Figure 4.8 The van't Hoff plot of ln KC vs 1/T for AR88 adsorption by PCS ...88

Figure 4.9 Regeneration of PCS on the adsorption and desorption of AR 88 dye solution ...89

Figure 4.10 The effect of mass ratio between N and T on adsorptive uptake and photocatalytic activity of AR88 and MB at initial dye concentration of 50 mg L^{-1} ...91

Figure 4.11 The effect of mass ratio between NT and PCS on adsorptive uptake and photocatalytic activity of (a) AR 88 and (b) MB, at initial dye concentration of 50 mg L^{-1} ...93

Figure 4.12 SEM images of (a) TiO_2, (b) NT, (c) NTP and (d) NTP after photocatalysis at 10000× magnification and EDX analysis of (e) TiO_2, (f) NT, (g) NTP and (h) NTP after photocatalysis at 10 000× magnification...95

Figure 4.13 FTIR results of (a) TiO_2, (b) NT and (c) NTP ...97

Figure 4.14 Absorbance UV/vis spectra of TiO_2, NT and NTP ...100

Figure 4.15 Band gap estimation using Tauc plot and Kubeka Munk function ..100

Figure 4.16 X-ray diffractograms of TiO_2, NT and NTP ...1071

Figure 4.17 Thermogravimetric and derivative weight loss of (a) TiO_2 and (b) NTP ...103

Figure 4.18 XPS spectra of (a) NTP, (b) C 1s spectra, (c) O 1s spectra, (d) Ti 2p spectra, (e) N 1s spectra and (f) P 2p spectra of NTP ...105

Figure 4.19 pH point of zero charge (pH_{pzc}) of (a) NTP1 and (b) NTP2 ...106

Figure 4.20 Control experiment for the adsorptive uptake and photocatalytic activity of MB and AR 88 by TiO_2, CS, PCS, NT and NTP at initial dye concentration of 50 mg L^{-1} and contact time of 120 mins.....108

Figure 4.21 Effect of initial pH solution on photocatalytic activity of (a) MB and (b) AR 88, at initial dye concentration of 50 mg L^{-1} ...110

Figure 4.22 Effect of initial pH solution on photocatalytic activity of (a) MB and (b) AR 88, at initial dye concentration of 50 mg L^{-1} ...113

Figure 4.23 Effect of initial concentrations of (a) MB and (b) AR 88 dye 115

Figure 4.24 Kinetics of photodegradation of (a) MB and (b) AR 88 dye using NTP at optimized conditions.....118

Figure 4.25 Langmuir-Hisenwoold model of both MB and AR 88 dye solutions, with different concentrations 119

Figure 4.26 Regeneration efficiency of NTP1 and NTP2 for MB and AR 88 dye, respectively, at initial dye concentration of 50 mg L^{-1}.....1710

Figure 4.27 Removal efficiency of MB and AR 88 dye solution by NTP under the presence of different quencher solutions, at 50 mg L^{-1}.....1271

Figure 4.28 Mineralization of (a) MB and (b) AR 88 dye by TOC/TOC_o values.....1714

Figure 4.29 Mineralization of (a) MB dye by the production of nitrate ions (b) AR 88 dye by the production of nitrate ions, (c) MB dye by the production of sulfate ions and (d) AR 88 dye by the production of sulfate ions, by NTP, TiO_2 and NT 1717

LIST OF SYMBOLS

Ebg	energy band gap
eV	band gap
K	equilibrium constant
k	rate of reaction constant
W	work functions
ΔG°	standard free energy
ΔH°	standard enthalpy change
ΔS°	standard entropy change
λ	absorption edge

LIST OF ABBREVIATIONS

1,4 BQ	1,4-benzoquinone
AOPs	Advanced oxidation processes
AR 88	Acid Red 88
BET	Brunauer-Emmett-Teller
BJH	Barrett-Joyner-Halenda
CB	conduction band
CS	Chitosan
DD	degree of deacetylation
Ebg	energy band gap
ED	electric field
EDTA	Ethylenediamine
EF	Fermi energy levels
ET	electron transfer
FTIR	Fourier-transform infrared spectroscopy
GLA	glutaraldehyde
HOMO	highest occupied molecular orbital
IPA	isopropyl alcohol
LUMO	lowest unoccupied molecular orbital
MB	Methylene Blue
MW	molecular weight
NIR	near-infrared
NT	nitrogen-doped TiO_2
NTP	nitrogen doped titania-phosphorylated chitosan
OH·	Hydroxyl radicals
OH_{ads}	adsorbed hydroxyl radical
PCS	Phosphorylated chitosan
pzc	pH at the point of zero charge
ROS	reactive oxygen species
SDG	Sustainable Development Goals
SEM-EDX	scanning electron microscopy-energy dispersive X-Ray analysis
TGA	thermogravimetric analysis

UV	Ultraviolet
UV-Vis DRS	UV–Vis diffuse reflectance spectroscopy
VB	valence band
XPS	X-ray photoelectron spectroscopy
XRD	X-ray powder diffraction

LIST OF APPENDICES

APPENDIX A EDX SPECTRUM

NITROGEN TERDOPKAN TITANIA-FOSFORILAT KITOSAN UNTUK DEKONTAMINASI PEMFOTOMANGKIN PEWARNA SINTETIK

ABSTRAK

Tujuan penyelidikan ini adalah untuk membangunkan fotopemangkin dwifungsi baharu yang terdiri daripada nanokomposit nitrogen terdop-titania (N-terdop TiO_2) dan fosforilat kitosan (PCS) untuk penyingkiran Asid Merah 88 (AR 88) dan Metilena Biru (MB) dari larutan akueus. Fosforilat kitosan telah berjaya diubahsuai melalui rawatan solvoterma menggunakan asid fosforik dalam autoklaf keluli tahan karat berlapis Teflon. Selepas itu, PCS yang diperolehi telah digabungkan dengan N-terdop TiO_2 untuk menyintesis nanokomposit N-terdop TiO_2-fosforilat kitosan (NTP) melalui rawatan solvoterma. Fotomangkin yang disintesis telah diperinci sepenuhnya menggunakan pelbagai teknik analitikal, termasuk mikroskop elektron pengimbasan dengan spektroskopi sinar-X penyebaran elektron (SEM-EDX), spektroskopi inframerah transformasi Fourier (FTIR), spektroskopi UV-Vis pantulan resapan (UV-Vis DRS), analisis Brunauer-Emmett- Teller (BET), analisis pembelauan sinar-X (XRD), spektroskopi fotoelektron sinar-X (XPS), dan analisis termogravimetrik (TGA). Hasil analisis menunjukkan bahawa nanokomposit mempunyai peningkatan kawasan permukaan dan kumpulan berfungsi. Aktiviti fotopemangkinan NTP terhadap pewarna MB dan AR 88 paling baik diterangkan oleh model kinetik Langmuir-Hinshelwood. Selain itu, kajian pemulihan dan kebolehgunaan semula mempamerkan prestasi yang sangat baik bagi NTP sebagai fotopemangkin . Eksperimen pengaut radikal menggunakan pengaut seperti asid etilenediaminetetraasetik (EDTA) (pengaut h^+ r), alkohol isopropil (IPA) (pengaut •OH), dan 1,4- benzokuinon (BQ) (pengaut ion superoksida) menunjukkan bahawa

IPA secara signifikan merencat aktiviti fotomangkinan bagi kedua-dua pewarna MB dan AR 88 sebanyak 17.9% dan 10% masing-masing. Oleh itu, disahkan bahawa spesies •OH hadir secara aktif semasa proses fotopemangkinan. Kajian mineralisasi yang dijalankan menggunakan analisis jumlah karbon organik (TOC) dan kromatografi ion (IC) menunjukkan peningkatan mineralisasi bagi MB dan AR 88 apabila dirawat dengan NTP. Secara kesuluruhan , fotopemangkin NTP yang disintesis telah menunjukkan prestasi yang menjanjikan untuk penguraian kedua-dua pewarna kationik dan anionik disebabkan oleh sifat sinergistik penjerapan-fotopemangkinannya.

NITROGEN DOPED TITANIA-PHOSPHORYLATED CHITOSAN FOR THE PHOTOCATALYTIC DECONTAMINATION OF SYNTHETIC DYES

ABSTRACT

The aim of this research is to develop a novel bifunctional photocatalyst composed of nitrogen-doped titania (N-doped TiO_2) and phosphorylated chitosan (PCS) nanocomposite for the removal of Acid Red 88 (AR 88) and Methylene Blue (MB) from aqueous solutions. Phosphorylation of chitosan was successfully modified through solvothermal treatment using phosphoric acid in a closed Teflon-lined stainless-steel autoclave. Subsequently, the obtained PCS was incorporated with N-doped TiO2 to synthesize the N-doped TiO2-phosphorylated chitosan (NTP) nanocomposite via solvothermal treatment. The synthesized photocatalyst was thoroughly characterized using various analytical techniques, including scanning electron microscopy with electron dispersive X-ray spectroscopy (SEM-EDX), Fourier-transform infrared spectroscopy (FTIR), UV–Vis diffuse reflectance spectroscopy (UV-Vis DRS), Brunauer-Emmett-Teller (BET) analysis, X-ray diffraction analysis (XRD), X-ray photoelectron spectroscopy (XPS), and thermogravimetric analysis (TGA). Results indicated that the nanocomposite exhibited enhanced surface area and functional groups. The photocatalytic activity of NTP towards MB and AR 88 dyes were best described by the Langmuir-Hinshelwood kinetic model. Furthermore, regeneration and reusability studies demonstrated the excellent performance of NTP as a photocatalyst. Radical scavenging experiments using scavengers such as ethylenediaminetetraacetic acid (EDTA) (h+ scavenger), isopropyl alcohol (IPA) (•OH scavenger), and 1,4-benzoquinone (BQ) (superoxide ions quencher) revealed that IPA significantly inhibited the photocatalytic activity of

both MB and AR 88 dyes by 17.9% and 10%, respectively. Therefore, it was confirmed that •OH species were actively present during the photocatalysis process. Mineralization studies conducted using total organic carbon (TOC) and ionic chromatography (IC) analyses showed enhanced mineralization of MB and AR 88 when treated with NTP . Overall, the synthesized NTP photocatalyst demonstrated promising performance in degrading both cationic and anionic dyes due to its synergistic adsorption-photocatalytic properties.

CHAPTER 1

INTRODUCTION

1.1 Overview

Water is the most important natural resource as every single life on the surface of earth depends on water as a means of growth and life, agriculture, food and drink, and energy (Al-Taai, 2021). It is very crucial to have a good water quality to satisfy the needs of society for clean water as poor water quality becomes a major contributor in water scarcity (Alcamo, 2019). However, due to social and economic development, the rise in water pollution has become major concern worldwide. The term: water pollution can be defined as the modification of water by one or more substances via a negative approach and are later discharged in it (Crini & Lichtfouse, 2019). Wastewater with effluents such as heavy metals, dyes, pesticides, herbicides, pharmaceuticals, cosmetics, oils, and organic compounds are discarded in the water without any further treatment. As a consequence, it can harm not only humans but the aquatic biota and environment as well. Water pollution can be classified into two categories: pollutants which belonged to a single origin such as industrial emissions into the water body, and, pollutants that are emitted from various origins (Crini & Lichtfouse, 2019). Pollutants from the industrial sources are one of the most critical pollutants after radioactive pollutants because most factories do not adhere to industrial drainage controls by using pesticides and fertilizers (Al-Taai, 2021).

Sustainable Development Goals (SDGs) is defined as development that meets the needs of the present without compromising the ability of future generations to meet their own needs (Holden et al., 2014). It is comprised of 17 SDGs which focuses on environmental protection, while providing economic and social development and welfare to present and future generations (Hansmann et al., 2012). One of the goals

under SDG is SDG 6: Clean Water and Sanitation, which aims to improve the quality of water by reducing pollution, discarding dumping and reducing the release of hazardous and poisonous chemicals and materials, cutting the proportion of untreated wastewater into half, and substantially increasing recycling and reusability worldwide (Alcamo, 2019). As such, various method has been introduced to solve this crisis including advanced oxidation processes (AOPs), adsorption, oxidations and filtrations.

The textile industry is one of the principal industries for the economic growth of a country and is considered the industry that conducts anthropogenic activities which take up a huge amount of water. However, it is a shame that the same industry brings about adverse effects to the environment as well as the living beings. Some of the pollution that is produced by the textile industry are dye pollution and air pollution, and among these two pollutions, dye pollution is a critical environmental problem since the dyeing process is the utmost significant technique in manufacturing (Yaseen & Scholz, 2019). An estimated mass of 700, 000 tons of different synthetic colorants was produced in a mass by the textile industry, annually, worldwide (Piaskowski et. al., 2018). As such, the dye effluent can greatly reduce the oxygen concentration because of the presence of hydrosulfide which blocks the passage of light into the water body (Parvin et. al., 2020).

Dyes can be manufactured from natural or synthetic resources. However, most of the textile industries use synthetic dyes compared to that of naturals due to their magnificent and brilliant color. Synthetic colorants are usually easy to detect with naked eyes, but it is quite challenging to eliminate them from the wastewater due to their aromatic chemical structure (Piaskowski et. al., 2018). Among the synthetic dyes that are widely used in the industry are acid, basic, direct, disperse, mordant, reactive,

sulfur, thiazine, azo and vat dyes (Bahrudin & Nawi, 2019). Among these dyes, vat and disperse dyes are insoluble in water. There are several categories of synthetic dyes that can be categorized, based on their chemical structure as well as chromophores or auxochrome groups including sulfur, azo, indigo, anthraquinone triphenylmethyl and phthalocyanine derivatives (Piaskowski et. al., 2018). Auxochrome plays an important role in elevating the dye color intensity. This auxotrophic group which is relatively polar has the property of fixing the color to the material is related to and can bind to the polar group of the fiber of the textiles (Lellis et. al., 2019).

Among the water contamination factors, synthetic dyes, which are a significant pollutant (Zhu et. al., 2012), are among the water contamination factors, due to their complete degree of fixation to the fiber during the dyeing and finishing process (Pang & Abdullah, 2013). It is mainly comprised of organic molecules are made from synthetic resources namely chemicals, petroleum by-products, and earth minerals (Ziarani et. al., 2018). Synthetic dyes have the tendency to become environmental recalcitrant and bioaccumulating dyes in soil and sediments, which then later transport them to public water supply system (Lellis et. al., 2019). Despite being a recalcitrant towards the aerobic environment, these synthetic colorants can be partially transformed or degraded in the presence of anoxic sediments, introducing the threatening aromatic amines (Lellis et. al., 2019). Besides, when dyes are combined with intermediate synthetic compounds, the generation of mutagenic and carcinogenic substances will be occurred (Lellis et. al., 2019). Even though synthetic dyes are available at low cost, it is proven to be hazardous to the water stream and environment due to their non-biodegradable property (Affat, 2021).

There are various methods that are used for dye removal which includes physical, chemical and biological method. Under physical treatment technology, method include reverse osmosis, forward osmosis, nanofiltration, microfiltration and electrodialysis are applied based on their respective principles (Ayush et. al., 2021). By using physical methods in treating wastewater, solids contain in effluent are eliminated either by flowing through filters or screens, or, by gravity settling or air flotation (Ayush et. al., 2021). Biological method in treating wastewater is designed to decontaminate pollutants in effluent based on the activated sludge of various aerobic and anaerobic microorganisms such as bacteria, green algae and fungi (Donkadokula et. al., 2020). Microorganisms play a vital role in attacking the organic pollutants by utilizing the organic contaminants as their nutrients to reproduce and live (Donkadokula et. al., 2020). On the other hand, chemical treatment of wastewater can be achieved by adding chemicals in a reacting system to facilitate the decontamination wastewater process (Ahmed et. al., 2021). Chemical process is considered the efficient method among others as it can be able to separate the dissolved pollutants in effluents, effectively, by adding targeted substances (Ahmed et. al., 2021). Both physical and biological methods cannot be applied in treating certain wastewater as the treatments are not sufficient to allow the treated water to enter water bodies (Ahmed et. al., 2021). As such, chemical treatment is the best process in treating wastewater. There are many processes that are listed under the chemical processes of treating wastewater including, ion-exchange, disinfection, ozonation, oxidation, advanced oxidation process, chemical precipitation, adsorption, neutralization and disinfection (Ahmed et. al., 2021; Samer, 2015). Among the processes, adsorption is the most simple, inexpensive and environmentally-friendly and an effective technique. The most important parameter in adsorption system is the isotherm, which describes the relationship

between the concentration of the adsorbent and the adsorption capacity of the adsorbent (Hosseini et. al., 2019). However, adsorption process has several limitations, including costly adsorbent, difficult in separating adsorbent from dye and possess low surface area (Moosavi et. al., 2020).

Advanced oxidation processes (AOPs) are an environmentally-friendly method that can able to remove various of pollutants such as water pollutants, dyes, air pollutants, hydrocarbons, petroleum-based contents, insecticides, pesticides, volatile organic compounds (VOCs) and other organic contaminants (Ameta et. al., 2018). The main objective of using AOPs in treating wastewater is to generate hydroxyl radicals (OH•) as a strong oxidant to eliminate any organic compounds that cannot be oxidized by any other conventional oxidants (Saravanan et. al., 2017).

Among the processes, heterogeneous photocatalysis is well-known in the industry and research due to its environmentally friendly approach and its capability of destroying organic compounds in effluents. Photocatalysis takes place by utilizing light and with the use of semiconductors. In spite of that, titanium dioxide (TiO_2) gained ample of attention in research activities due to its biocompatibility, low-cost, wide availability, non-toxicity and high chemical stability (Haider *et. al.*, 2019). In fact, it has the capability to absorb the incoming photons. TiO_2 is a commonly used semiconductor, besides zinc oxide (ZnO), iron oxide (Fe_3O_4), copper oxide (CuO), aluminum oxide (Al_2O_3), vanadium (IV) oxide and niobium (IV) oxide (Nb_2O_5). Among the semiconductors, TiO_2 is favored due to its non-toxicity, stability, oxidative ability, and solar activation (Nasirian & Mehrvar, 2016). Its electronic configuration consists of an empty conduction band, filled valence band and an energetic gap (Nasirian & Mehrvar, 2016). However, due to the low surface area and wide band gap

energy (3.2 eV), TiO_2 is less efficient during photocatalytic reaction and can only be activated under UV irradiation. Therefore, in order to improve the photocatalytic activity of TiO_2, metal ions (noble or transition metals) or non-metal ion doping is introduced. Doping of TiO_2 with metal ions aids in increasing its surface area and as well as its photoactivity. Selecting a dopant is very important to determine the overall photocatalytic activity of TiO_2 (Park et. al., 2013).

Chitosan (CS) is the second most abundant in polysaccharide in nature after cellulose. It is highly biodegradable, non-toxic, environmentally friendly, biocompatible and has high adsorption capacity. CS is obtained through the deacetylation of chitin under alkaline conditions. The presence of pendant hydroxyl group and free amino group in the structure of CS contributes active adsorption sites. As a versatile biopolymer, CS play an immense role in wastewater treatment. Nevertheless, the performance of CS as an adsorbent is limited due to its poor chemical stability, weak mechanical strength and low adsorption capacity in its pristine form. As such, an effective modification of CS can be able to improve its adsorption capability, selectivity, mechanical strength and chemical stability. The physiochemical properties of CS will be altered after some modifications, which will affect its behavior in adsorption process (Wang & Zhuang, 2017). Several factors have to be taken into account namely molecular weight (MW), conditions of reaction and viscosity of CS (Azmana *et. al.*, 2021). There are three types of modifications of CS including physical and chemical modifications. Among these two, physical modification of CS is the easiest method. Physical modification of CS is time effective, feasible and economical compared to the other two methods (Azmana *et. al.*, 2021). Example of physical modification is by blending or mixing two polymers to create a new material to enable molecular interactions. Chemical modifications on the other hand play a major role in

elevating the reactive functional groups present in CS. The chemical modification of CS does not change the structure of the molecule. Some examples of chemical modifications of CS include phosphorylation, thiolation, sulfonation, hydroxyalkylation, carboxyalkylation, alkylation, quaternization and graft copolymerization (Azmana *et. al.,* 2021). Biological modification of CS is performed through enzymatic modification. The main benefit in performing this modification is due to its specificity and environmental benefits (Azmana *et. al.,* 2021). Recently, chitosan-based nanocomposite coated fiber (ZnO-CS) was developed for wastewater treatment showing a high degree of photocatalytic activity of Rhodamine B (Karthik *et.al.,* 2023). Despite that, more studies are required in order to enhance the applications of CS in wastewater treatment including selecting appropriate materials for the composites, finding simple and eco-friendly ways to make nanocomposites using selected materials, and optimizing different factors affecting its synthesis and adsorption (Karthik *et.al.,* 2023).

1.2 Problem statement

Despite having a great number of advantages, TiO_2 has its own drawbacks, which restricts its applications in photocatalytic activities. One of the issues is the low adsorption ability of TiO_2 photocatalyst for pollutants, thus reducing its efficiency in treating effluents. Current research trends show a growing interest in visible light photocatalysis for various treatments. However, due to wide band gap energy, TiO_2 requires ultraviolet (UV) to initiate the photocatalytic activity. Besides, the non-doped TiO_2 is reported to be inefficient due to its relatively low reduction potential of electrons (-0.5 V) in the conduction band (CB) of TiO_2 compared to the theoretical thermodynamic requirement (Al Jitan et. al., 2020). Apart from that, the presence of

strong reducing electrons and free radicals is quite destructive as it can lead to the formation of molecular hydrogen (Al Jitan et. al., 2020). Doping of TiO_2 especially with non-metals can increase the light absorption of TiO_2 into visible light and preventing agglomeration of TiO_2 nanoparticles, but the performance of visible light activity of non-metal doped TiO_2 is relatively low compared to non-doped TiO_2 under UV irradiation (Dong, et.al., 2011). Moreover, non-metal doping can act as recombination centers, limiting electron-hole separation.

To overcome this issue, CS may incorporate on the surface of TiO_2 to increase the adsorption capability, as CS is known for its effectiveness in adsorbing organic materials, dyes, and heavy metals in effluent treatment (Nawi, et.al., 2010). Modification of CS through phosphorylation can serve as an alternative method for producing improved functional materials. The choice of non-metal dopants is important in overcoming the drawbacks. Among the non-metal dopants, N-doped TiO_2 exhibit a significant photocatalytic activity and strong absorption various reactions under visible light irradiation, where both of the N impurity and Ti^{3+} act cooperatively to narrow the band gap of N-doped TiO_2 (H. Li et. al., 2015). Apart from that, the hybrid system employment on TiO_2 will help to enhance its behavior. Hybridization of TiO_2, a technique where two or more different modification techniques are applied, can further enhance its performance. Recent studies have shown promising results with TiO_2-CS hybrid composites, such as the adsorption of copper (II) ions (Su et. al.,2022), indicating the potential for addressing the limitations of TiO_2.

1.3 Research objectives

In order to overcome the shortcomings, the objective of the study is to design a new method for the fabrication of effective N-doped TiO_2 / phosphorylated chitosan as a hybrid nanocomposite with high sustainability, low-cost and eco-friendly. Therefore, the objectives of the study are:

1. To synthesize a novel bifunctional nanocomposite of N-doped TiO_2-phosphorylated chitosan by the solvothermal method and optimize the mass ratio of the adsorbent and N-doped titania.
2. To characterize the synthesized nanocomposite for its physical, chemical and optical properties using various characterization techniques.
3. To evaluate the adsorption and photocatalytic performance of the nanocomposite for the removal of synthetic dyes from aqueous solution using the Langmuir-Hinshelwood kinetic model.
4. To investigate the reusability of the nanocomposite upon regeneration and assess its mineralization using total organic carbon (TOC) values and ionic chromatography (IC) analysis.

1.4 Scope of study

This research focused on the novel method of fabricating nitrogen doped titania-phosphorylated chitosan (NTP) and to evaluate the synergistic effect of adsorption-photocatalysis for the removal of different dyes (AR88 and MB) from aqueous solution. Phosphorylated chitosan (PCS) is first synthesized to evaluate its adsorption performance. The adsorption studies focused on the effect of pH solution (3-11), initial dye concentration (20 - 100 mg L^{-1}) and contact time. Adsorption

isotherm (Langmuir, Freundlich and Temkin) and kinetic (pseudo-first order and pseudo-second order rate) models were applied in this adsorptive uptake studies to investigate the equilibrium and kinetics data. In addition, the adsorption studies of PCS were also focused on the effect of temperature (30 - 50°C) to accessed the thermodynamic parameters including change in free energy (ΔG°), change in entropy (ΔS°) and change in enthalpy (ΔH°). The synergistic adsorption-photocatalytic performance of NTP for dyes removal focused on the mass ratio between photocatalyst and adsorbent, effect of dosage, pH solution (3-10), initial dye concentration (30 - 200 mg L^{-1}) and contact time. Characterizations including Fourier-transform infrared spectroscopy (FTIR), scanning electron microscopy-energy dispersive X-Ray analysis (SEM-EDX), UV–Vis diffuse reflectance spectroscopy (UV-Vis DRS), X-ray powder diffraction (XRD), Brunauer-Emmett-Teller (BET), X-ray photoelectron spectroscopy (XPS), thermogravimetric analysis (TGA), photoluminescence analysis (PL) and pH at the point of zero charge (pH_{pzc}), were conducted in order to identify the physical, chemical and optical properties of the prepared composite. Besides, the effect of radical scavengers was evaluated by using different types of scavengers in order to determine the •OH radicals production route. Finally, mineralization study was conducted using total organic carbon (TOC) and ion chromatography (IC) analysis..

1.5 Outline of thesis

There are five chapters comprised in this thesis, including Chapter 1: General introduction, Chapter 2: Collecting and study information, facts and theories, Chapter 3: General materials and method, Chapter 4: Discussion of obtained results and Chapter 5: Conclusion of the study.

CHAPTER 2

LITERATURE REVIEW

2.1 Advanced oxidation processes

Advanced oxidation process (AOP) can be defined as the oxidation processes related to the generation of reactive oxygen species (ROS) such as hydroxyl radicals (•OH) in enough quantity to produce reclaimed effluents (Garrido-Cardenas et. al., 2020). AOP is operated by generating reactive species such as hydroxyl radicals (•OH), superoxide anion radicals (O2•-), hyperoxide radicals (•O2H) and sulphate radicals (SO4•-) in order to oxidize the organic contaminants, yielding carbon dioxide (CO2), water (H2O) and inorganic ions as final products (Ribeiro et. al., 2015). The generated free radicals are superiorly reactive due to their unpaired electrons, which greatly contribute to the water purification process. The unpaired electrons of •OH radicals have short lifetimes, making them actively react to a series of chemical species. During wastewater application, these radicals act as a powerful oxidizing agent to decontaminate emerging pollutants from the water and modify the captured pollutants into less toxic products (Deng & Zhao, 2015).

Generally, AOPs can be classified into two groups namely non-photochemical AOPs and photochemical AOPs. Non-photochemical AOPs include ozonation, ozone/hydrogen peroxide, Fenton, Fenton-like process, cavitation and wet air oxidation (Saravanan et. al., 2017). On the other hand, photochemical AOPs include homogeneous and heterogeneous photocatalysis, photo-Fenton, UV/hydrogen peroxide, UV/ ozone, and UV/hydrogen peroxide/ozone (Saravanan et. al., 2017) (Figure 2.1). The main mechanism of AOP is the utilization of light energy, where, soon as the light energy is sparked onto the catalyst's surface, the vibration of valence band electrons induced. The electrons from the valence band are then excited to the

conduction band, resulting in the formation of holes in the valence band of the catalyst. The holes in the valence band can oxidize donor atoms or molecules and react with water molecules to produce •OH radicals. As such, the oxidation reaction of the •OH radicals with the effluents produces biodegradable intermediates (Saravanan et. al., 2017).

The •OH radical is the most important component in the degradation of effluents. It is the most reactive oxidizing agent with an oxidation potential of 2.8 eV (Ameta et. al., 2018). It has non-selective characteristics which attack emerging organic contaminants by four routes namely radical addition, hydrogen abstraction, electron transfer, and radical combination, resulting in carbon-centered radicals (R•) which can be transformed into organic peroxyl radicals (ROO•) (Deng & Zhao, 2015). The advantages and disadvantages of AOP vary according the type of processes involved. Table 2.1 summarizes the advantages and disadvantages of various AOP.

Table 2.1 The advantages and disadvantages of various AOP (Brienza & Katsoyiannis, 2017).

AOP	**Advantages**	**Disadvantages**
Fenton's reaction	• Able to degrade soluble and insoluble dyes in industrial effluents. • No potential formation of bromated by-product.	• Iron sludge generation due to combined flocculation of the reagent and the organic compounds. • Low pH (< 2.5) is required to keep iron in solution. • pH adjustment will increase operating cost.

TiO_2 catalyzed UV oxidation	• No potential formation of bromated by-product. • Recycling of the catalysts. • Performance also at higher wavelengths and under solar irradiation.	• No full-scale application exists. • If the catalyst is added as a slurry, separation step is required. • Adapted and optimum concentration of catalyst required a rigorous study.
H_2O_2/O_3	• Formation of strong non-selective hydroxyl radicals that are able to break down the conjugated double bond. • Ozone can be used in its gaseous state and consequently does not raise the volume of wastewater. • No sludge generation.	• Low rate of degradation as equated to the AOP processes due to less production of hydroxyl radicals. • Ozone may form toxic by- products. • High cost. • Requires treatment of access H_2O_2 due to potential for microbial growth.
O_3/UV	• More efficient than O_3 or UV alone. • Disinfectant. • For equal oxidant concentration, more efficient at generating hydroxyl radical than H_2O_2/UV.	• Potential bromated by product. • UV light penetration can be obstructed by turbidity. • Compounds such as nitrate can interfere with the absorbance of UV light. • Energy and cost intensive processes.

H_2O_2/UV	• No potential formation of bromated compounds. • Full scale drinking water treatment system exists.	• Potential bromated by product. • UV light penetration can be obstructed by turbidity. • Compounds such as nitrate can interfere with absorbance of UV light.
Sonication	• Less heat transfer relative to UV system. • No bromated formation if O_3 is not added.	• No full-scale application exists. • Oxidant may be needed to improve the efficiency of the treatment, thereby increasing cost.

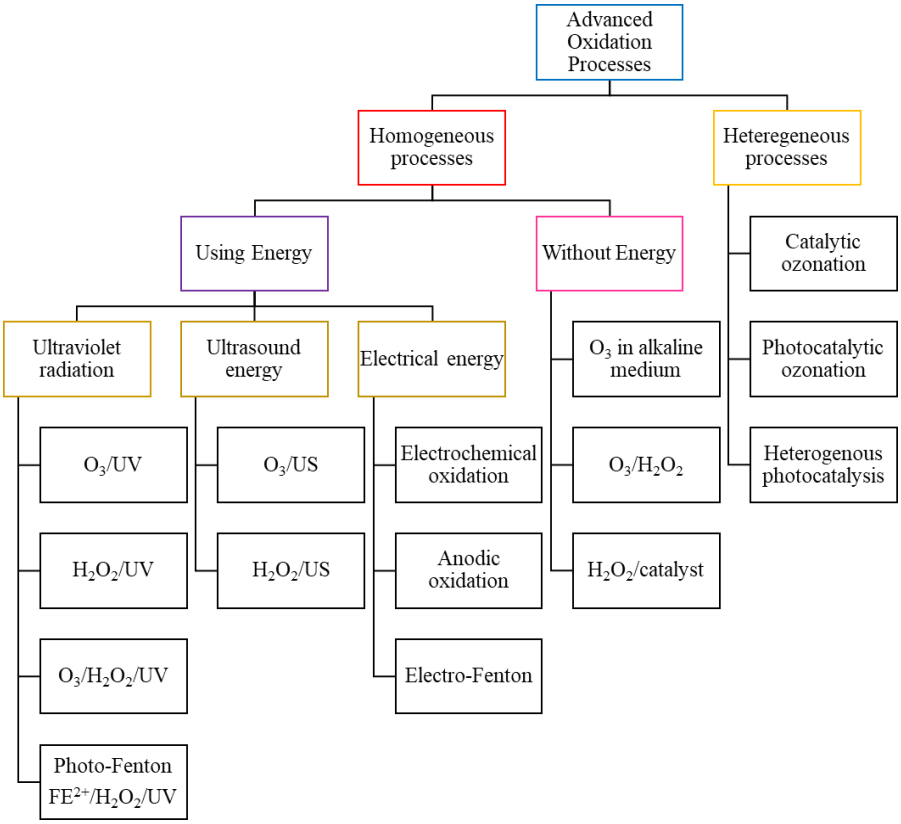

Figure 2.1 Classifications of AOPs (Poyatos *et. al.*, 2010).

2.1.1 Photocatalysis

Photocatalysis is one of the AOPs which consist of photocatalyst to harvest sunlight. It can be defined as catalysis driven acceleration of a light-induced reaction (Saravanan *et. al.*, 2017). Photocatalyst, also known as semiconductor, is a material that changes the chemical reaction rate under exposure of light, where the phenomenon is known as photocatalysis (Ameta *et. al.*, 2018). Being a substrate, photocatalyst absorbs light and plays a vital role as catalyst for chemical reactions. Photocatalysis uses solar energy to oxidize pollutants by triggering electron excitation transfer in a photocatalyst (Antonopoulou *et. al.*, 2021). During this phenomenon, electron-hole pair is produced when the semiconductor photocatalyst is exposed towards light. The photocatalysis process can be categorized into two processes according to the

appearance and physical state of reactants (Ameta *et. al.*, 2018): homogenous and heterogeneous photocatalytic reactions. Homogeneous photocatalysis occurs when both the semiconductor and reactant are in the same phase, whereas, heterogeneous photocatalysis occurs when both the semiconductor and reactant are in different phases.

2.1.2 Principles of heterogeneous photocatalysis

Heterogeneous photocatalysis can be defined as the acceleration of photoreaction in the presence of a catalyst (Ibhadon & Fitzpatrick, 2013). At standard temperature and pressure, and in the presence of oxygen, heterogeneous photocatalysis employs semiconductor oxides illuminated with either UV or visible light (Loddo *et. al.*, 2018). The primary mechanism of the reaction is the formation of electron-hole pairs, which, once separated, govern the initiation of redox reactions of species adsorbed on the active surface (Loddo *et. al.*, 2018). The following are some of the most intriguing aspects of heterogeneous photocatalysis (Ahmed & Haider, 2018):

I. The contaminants totally breakdown into CO_2 and other inorganic compounds.
II. The operation is carried out in optimal conditions
III. The presence of oxygen and ultra-band gap energy, both of which can be obtained directly from the air and sun, are the sole prerequisites for the reaction to occur.
IV. The catalyst can be assisted on a variety of inert matrices, including glasses, nanotubes, polymers, graphene oxides and carbon.

V. The catalyst is a low-cost, non-toxic, and reusable material.

Heterogenous photocatalysis can be applied in various applications such as in cancer treatment, environmental, photocatalytic coatings, structural applications and in selective oxidation and reduction application, as shown in Figure 2.2. It is one of the environmentally friendly, highly efficient, have a good viability across a wide pH range and cost-efficient techniques. During the employment of the technique, the solid catalyst is usually either in slurry-type form which is suspended in the water effluent or is immobilized onto the surface of a variety of substrate types and configurations, making catalyst recovery and reusability quite easy (Foteinis & Chatzisymeon, 2020).

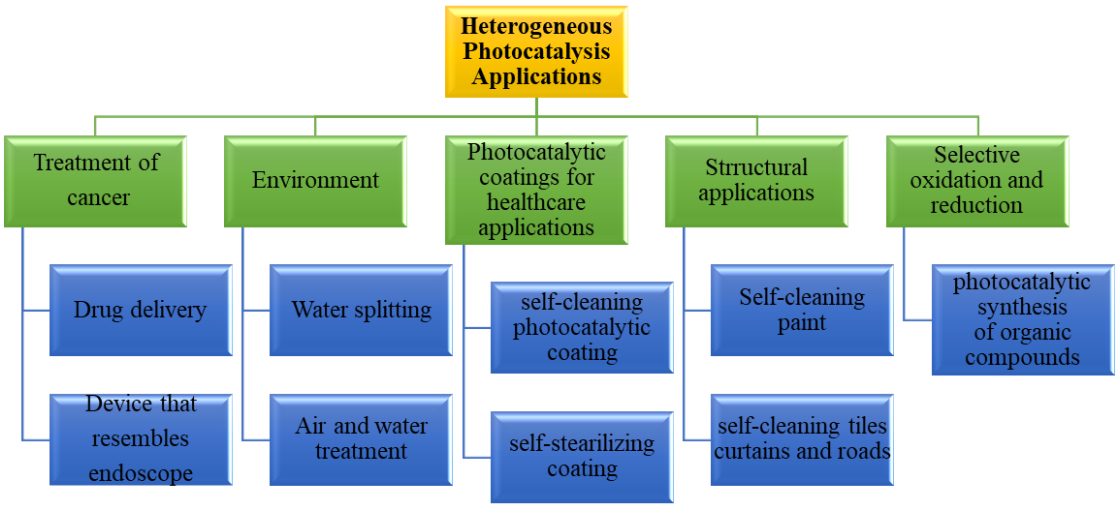

Figure 2.2 Heterogeneous photocatalysis applications (Ahmed & Haider, 2018)

The main mechanism that involves in heterogeneous photocatalysis are oxidative and reductive reactions on the photocatalyst's surface, in which the photocatalyst converts photons into chemical energy to be used in water treatment application (Foteinis & Chatzisymeon, 2020). The production, separation, recombination, and surface capture of photogenerated electrons and hole pairs are the essential processes in the photocatalytic process (Kang *et. al.*, 2019). A semiconductor

or photocatalyst has two energy bands known as the lowest occupied (valence band) and the highest unoccupied (conduction band) energy bands, which are divided by an energy band gap (E_{bg}), a closely spaced orbital (Ahmed & Haider, 2018). The energy band gap is very crucial in order to generate the electron hole pairs. Therefore, when a photocatalyst absorbs light energy that carries photon energy, which is greater than or equal to its E_{bg}, the electrons from the valence band (VB) got excited (photoexcitation) and are promoted to the conduction band (CB) in femtoseconds (Ahmed & Haider, 2018; Foteinis & Chatzisymeon, 2020). This phenomenon creates an unfilled VB, which generates a positive hole (h^+), producing an electron-hole pair (Ahmed & Haider, 2018).

The important factors that influenced the heterogeneous photocatalysis are temperature, water matrix, concentration of catalyst, the wavelength and the intensity of light, initial concentration of the substrate and pH. Therefore, these factors are very vital to be considered before conducting any photocatalytic activities.

2.1.3 Kinetic Modelling

Kinetic models are important for studying the mechanism and catalytic performances (Hai *et.al.*, 2023). Some of the kinetic models that are applied in photocatalysis include the n^{th} order, Langmuir-Hinshelwood and Michaelis-Menden (Andrieux *et.al.*, 2011). Langmuir-Hinshelwood (L-H) kinetic model is an equation to describe the photocatalytic kinetics, where the oxidation rate is the limiting reaction rate at maximum coverage of catalyst (Molinari & Palmisano, 2010). It is also used to determine the relationship between initial degradation rate and the initial concentration of the organic substrate (Kumar *et.al.*, 2007).

L-H model is extensively applied in heterogeneous photocatalytic degradation of wastewater. It is used to characterize solid catalytic reactions which involves four main steps including adsorption of molecules on a catalytic surface, dissociation of adsorbed molecules, reactions of dissociated molecules to produce products, and desorption of products (Hai *et.al.,* 2023). The L-H model is commonly expressed as Equation 2.2 (Li *et.al.,* 2007):

$$r = -\frac{dC}{dt} = k_s \frac{K_r K_S C}{1+K_S C_0} = k_{app} C \tag{2.1}$$

$$\frac{1}{k_{app}} = \frac{1}{k_r K_S} + \frac{C_0}{k_r} \tag{2.2}$$

where k_{app} is the apparent first-order rate constant, t is the reaction time, C_0 is the initial organic content, k_r is the reaction rate constant and K_S is the adsorption rate constant.

From the expression above, the reaction rate, k_r, is dependent on the light intensity and adsorption performance of the catalyst (Li *et.al.,* 2007). The L-H kinetic model is quite compatible in kinetic data for photocatalytic degradation studies according to previous reports. Recently, a research work on the photocatalytic degradation of ester-105 by La/TiO_2 was well-conformed with L-H kinetic model, which provides a theoretical foundation in industrial application (Zhu *et.al.,* 2023).

2.2 Adsorption

Adsorption is a process where organic substances from a liquid phase are transferred onto the surface of a solid phase. The adsorption on the solid surface is that the molecules or atoms on the solid surface have residual surface energy due to unbalanced forces. When some substances collide with the solid surface, they are attracted by these unbalanced forces and stay on the solid surface (Hu & Xu, 2020).

Compared to all the conventional methods in treating wastewater, adsorption technique appears to the forefront as a result of its operation flexibility, design processes and gives a significant effect on toxicity, biological availability and transport of heavy metals in effluents (Chai *et.al.,* 2021). This method is not only cost-effective and environmentally-friendly but as well as highly effective treatment method where the removal efficiency of adsorptive uptake can range up to 99.9% (Rashid *et.al.,* 2021). During the adsorptive uptake, the adsorbate migrates according to the three following steps: 1) migration of adsorbate to the border shell of the adsorbent, 2) intraparticle diffusion into pores, and 3) adsorption and desorption of solute (Rashid *et.al.,* 2021).

Adsorption processes can be categorized into two types which are the physical and chemical adsorption. The physical adsorption of the effluents occurs in which the concentration of the adsorbate increase at the surface is due to non-specific van der Waals forces. Physical adsorption is generally reversible, weakly specific and has small thermal effect. On the other hand, the chemical adsorption or chemisorption of the adsorption process is caused by chemical reactions between the adsorbate and the adsorbent which create covalent or ionic bonds. It is mostly irreversible, selective and its heat ranges from tens to hundreds of kJ mol^{-1} (Burakov *et.al.,* 2018). Examples of common adsorbents include clay, biochar, alumina, zeolites, activated carbon and chitosan.

2.3 Titanium dioxide (TiO_2)

2.3.1 General

TiO_2, also well-known as titania or titanium (IV) oxide, belongs to the transition metal oxides (Haider et. al., 2019). It exists in white powder with three crystalline phases: anatase, brookite and rutile. It is commonly used in paint, cosmetics, paper, catalysts, rubber, ceramics, plastics, solar cells, water treatment, medicines, toothpastes, varnishes, food industries, electronic devices and as well as in sunscreens (Ali et. al., 2018; Haider et. al., 2019). Compared to other semiconductor materials, TiO_2 is inexpensive, changes its oxidation state but does not decompose at the same time, has high degradation efficiency, has high specific surface area, has rapid rate of reaction, low toxicity, biocompatible and as well as has simple preparation (Gopinath et. al., 2020). Besides, TiO_2 is highly favored in wastewater treatment due to its modifiable morphology including nanotubes, mesoporous surface which can aid in transferring ions within particles, high crystallinity and it does not decompose into hazardous substances unlike other photocatalysts do (Gopinath et. al., 2020).

2.3.2 Properties of TiO_2 semiconductor

TiO_2 is an efficient photocatalyst with a molecular weight of 79.866 g mol^{-1}. It is a cost-effective, biocompatible, chemically stable, low-toxicity and high thermal stability semiconductor by having a high photocatalytic activity and a strong oxidizing agent. It is typically, a n-type semiconductor as it possesses oxygen deficiency (Pelaez *et. al.*, 2012). Naturally, TiO_2 exists in the most common three polymorphs namely anatase, brookite and rutile. Other few common structures of TiO_2 include columbite, baddeleyite, ramsdellite, hollandite and monoclinic (Ali *et. al.*, 2018). Among the

polymorphs, rutile is the most stable form of TiO_2 but the anatase form of TiO_2 is mostly favored in photocatalysis process. In the laboratory, all three polymorphs are easily synthesized and usually, with calcination at temperatures above 600 ℃, the metastable anatase and brookite will change to the thermodynamically stable rutile (Pelaez *et. al.*, 2012). The band gap for anatase, brookite and rutile is 3.2 eV, 3.2 eV and 3.0 eV, respectively. Titanium (Ti^{4+}) atoms are coordinated to six oxygen (O_2) atoms in all three forms, resulting in TiO_6 octahedra (Pelaez *et. al.*, 2012). Among the forms, the most studied surfaces of TiO_2 are anatase form with (101) face and rutile form with (110) face. Anna and her co-workers (2018) have studied structural properties of TiO_2 nanomaterials by analyzing the semiconductor with different morphological especially on its surface states. The outcome of their study revealed that anatase is the predominant phase in all their investigated materials including spherical nanoparticles, nanocrystals and nanoflowers.

2.3.3 TiO_2 in photocatalysis

TiO_2 has been widely used as a photocatalyst for initiating a series of reductive and oxidative processes on its surface (Dong *et. al.*, 2015). In general, there are five fundamental steps involved in TiO_2 photocatalysis (Dong *et. al.*, 2015):

I. Photoexcitation, where the absorption of light and generation of charge carriers are happened
II. Diffusion
III. Trapping
IV. Recombination
V. Oxidation

Equation 2.3 below shows the photoexcitation mechanism of TiO_2 (Foteinis & Chatzisymeon, 2020):

$$\text{Photoexcitation: } TiO_2 + hv \rightarrow e^-_{CB}\ (TiO_2) + h^+_{VB}\ (TiO_2) \quad (2.3)$$

Once TiO_2 is irradiated with light energy, equivalent to or greater than the band gap, as shown in Equation 2.3, the electrons from the VB are excited and jumped to the CB (Figure 2.3), creating an electron-hole pair in both VB and CB (Dong *et. al.*, 2015; Magalhaes *et. al.*, 2017). If the obtained electrons and holes are entrapped on the surface of the photocatalyst and their recombination is averted, a series of chain of oxidation and reduction will be initiated (Equation 2.4 – 2.11) (Ahmed & Haider, 2018; Foteinis & Chatzisymeon, 2020; Loddo *et. al.*, 2018):

$$\text{Entrapment of free electrons: } e^-_{CB} \rightarrow e^-_{TR} \quad (2.4)$$

$$\text{Entrapment of holes: } h^+_{VB} \rightarrow h^+_{TR} \quad (2.5)$$

$$\text{Charge carrier recombination: } e^-_{TR} + h^+_{VB} \rightarrow e^-_{CB} + \text{heat} \quad (2.6)$$

$$\text{Oxidation of hydroxyls: } (OH^-)_{ads} + h^+ \rightarrow \bullet OH_{ads} \quad (2.7)$$

$$\text{Photoexcited electron scavenging: } (O_2)_{ads} + e^- \rightarrow O_2^{\bullet -} \quad (2.8)$$

$$\text{Protonation of superoxides: } O_2^{\bullet -} + \bullet OH \rightarrow HOO\bullet \quad (2.9)$$

$$\text{Co-scavenging of } e^-\text{: } HOO\bullet + e^- \rightarrow HO_2^{\bullet} \quad (2.10)$$

$$\text{Photodegradation by OH radicals: } R\text{-}H + OH\bullet \rightarrow R\bullet + H_2O \quad (2.11)$$

The e^-_{TR} and h^+_{TR} in above equations depict the surface trapped valence band electron and conduction band hole, respectively (Dong *et. al.*, 2015). In Equation 2.6, the photoexcited electron recombines with the valence band hole in nanoseconds without the presence of electron scavengers, dissipating heat energy concurrently. Therefore, the presence of electron scavengers is critical for extending recombination

and ensuring the successful operation of photocatalysis (Dong *et. al.*, 2015). Typically, the surface of OH groups on the TiO_2 particles react with the positive hole to form surface adsorbed hydroxyl radical ($\bullet OH_{ads}$). As such, Equation 2.7 and 2.8 show the prevention of recombination of electron-hole pairs under the presence of oxygen, while the formation of superoxide radical anion ($O^{\bullet -}$) occurs (Dong *et. al.*, 2015). The formation of $O_2^{\bullet -}$ anion can be then protonated to hydroperoxyl radical ($HO_2^{\bullet -}$) and later to hydrogen peroxide (H_2O_2). It should be taken note that Equation 2.7 and 2.12 play a major role in the water purification process. The overall final products of the heterogenous photocatalysis process are H_2O, CO_2 and intermediate products (Equation 2.12) (Foteinis & Chatzisymeon, 2020):

$$\text{R-H (pollutant)} \xrightarrow{TiO_2/h\nu} \text{intermediate (s)} \rightarrow CO_2 + H_2O + \text{inorganic ions} \qquad (2.12)$$

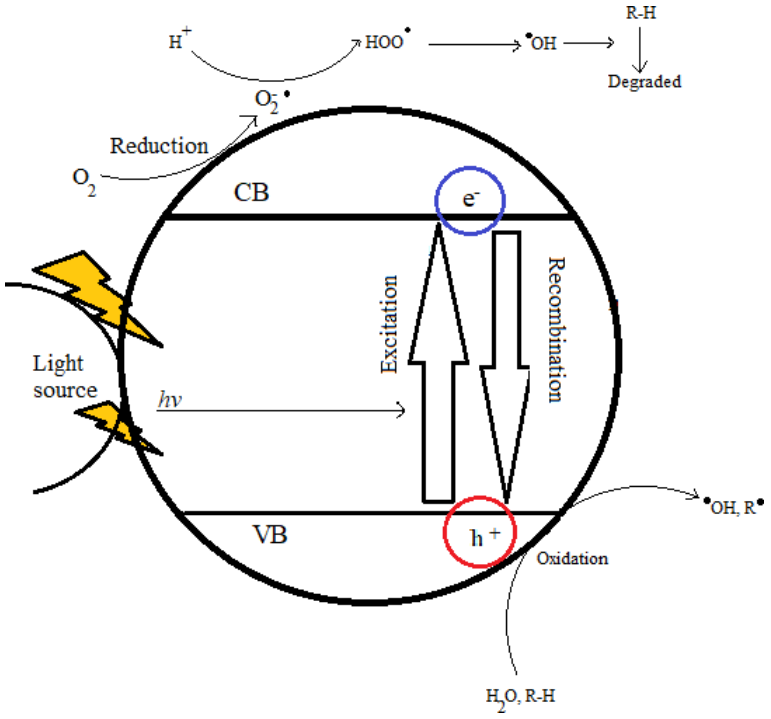

Figure 2.3 Illustration of photocatalytic activity of TiO_2 mechanism on pollutant (RH) (Dong *et. al.*, 2015).